

# Applicability of alternating phase shifting masks using polarized light

Karsten Bubke<sup>\*</sup>, Martin Sczyrba, Christophe Pierrat

Advanced Mask Technology Center GmbH & Co. KG, Raehntzer Allee 9, D-01109 Dresden,  
Germany

## ABSTRACT

The use of Alternating Phase Shifting Masks (APSM) for sub 50nm half pitch pattern using 193nm lithography was evaluated. Results show that polarized illumination may be necessary for APSM to compete with Half-Tone Phase-Shifting Masks (HTPSM) when printing sub 50nm features. The low sigma illumination conditions required for APSM constraints the choice of a possible polarized illuminator to the TE polarized option therefore limiting the patterns to be oriented in one direction.

Topography effects imply the use of polarization-dependant balancing of APSM which should not be a show-stopper as long as it is properly handled at the time the mask is manufactured. Due to topography effects, the MEEF is also increased if compared to thin mask approximation but the relative numbers remain manageable.

The sensitivity of CD errors with respect to polarization errors of the source is comparable to HTPSM masks. The induced displacement error due to polarization errors is small compared to the CD variation of the dark line.

Keywords: Alternating phase shift mask, balancing, immersion, polarized light high NA, immersion lithography

## 1. INTRODUCTION

Extension of 193nm optical lithography beyond the 65nm node will require the use of a variety of resolution enhancement techniques (RET) in combination with immersion technology and, most likely, polarized illumination. Implementation concepts and possible issues related to the use of polarized light have already been reported [1-5], and the first experimental results confirmed the potential of the technology [6,7]. The interaction of mask topography with polarized light has also been investigated both theoretically and experimentally [8-10].

One potential RET for the 45nm node and below is the application of Alternating Phase Shifting Masks (APSM) as they offer high resolution and low Mask Error Enhancement Factor (MEEF). However, the introduction of polarized light has made their advantages less obvious compared to other mask types.

The goal of this paper is to explore some of the benefits APSM might offer in combination with polarized light and point out the advantages and drawbacks of alternatives like Half Tone Phase-Shifting Masks (HTPSM).

First, we explore the applicability of APSM for sub 50nm half pitch printing in order to define the type of patterns that can be printed and the optimum illumination conditions. For these patterns, mask topography effects on MEEF as well as APSM balancing are addressed for polarized and un-polarized illumination in a second step. Finally, the influence of polarization errors on the imaging performance is discussed and compared with HTPSM masks.

## 2. APPLICABILITY OF APSM FOR SUB-50NM HALF PITCH PATTERNS

In what follows, we will compare the imaging properties of APSM and HTPSM with 6% transmission for dense lines and spaces by means of simple contrast and MEEF calculations. As we are interested in the inherent properties of the respective illumination schemes, we assume an infinitely thin mask (i.e. the Kirchhoff approximation). The impact of mask topography effects is examined in subsequent sections. The influence of the resist processing is neglected and we require that only the relevant orders, i.e. the 0<sup>th</sup> and first order, are completely captured by the pupil. Under these assumptions both MEEF and contrast of the resist image can be calculated analytically.

---

<sup>\*</sup> karsten.bubke@amtc-dresden.com, phone +49 351 4048 377, fax +49 351 4048 9377

The printing of dense lines and spaces at low k1 using binary masks or HTPSM requires off-axis illumination. In Fig. 1, four generic cases using polarized or un-polarized light which serve as a basis for the following investigations are depicted: (a) perfect dipole illumination for printing of lines in one direction (b) the corresponding version with polarized illumination, (c) quadrupole illumination for structures in two directions and (d) the counterpart with bipolar or azimuthal polarization. Whereas (a) and (b) are typical double exposure options, (c) and (d) can be considered as single exposure options.

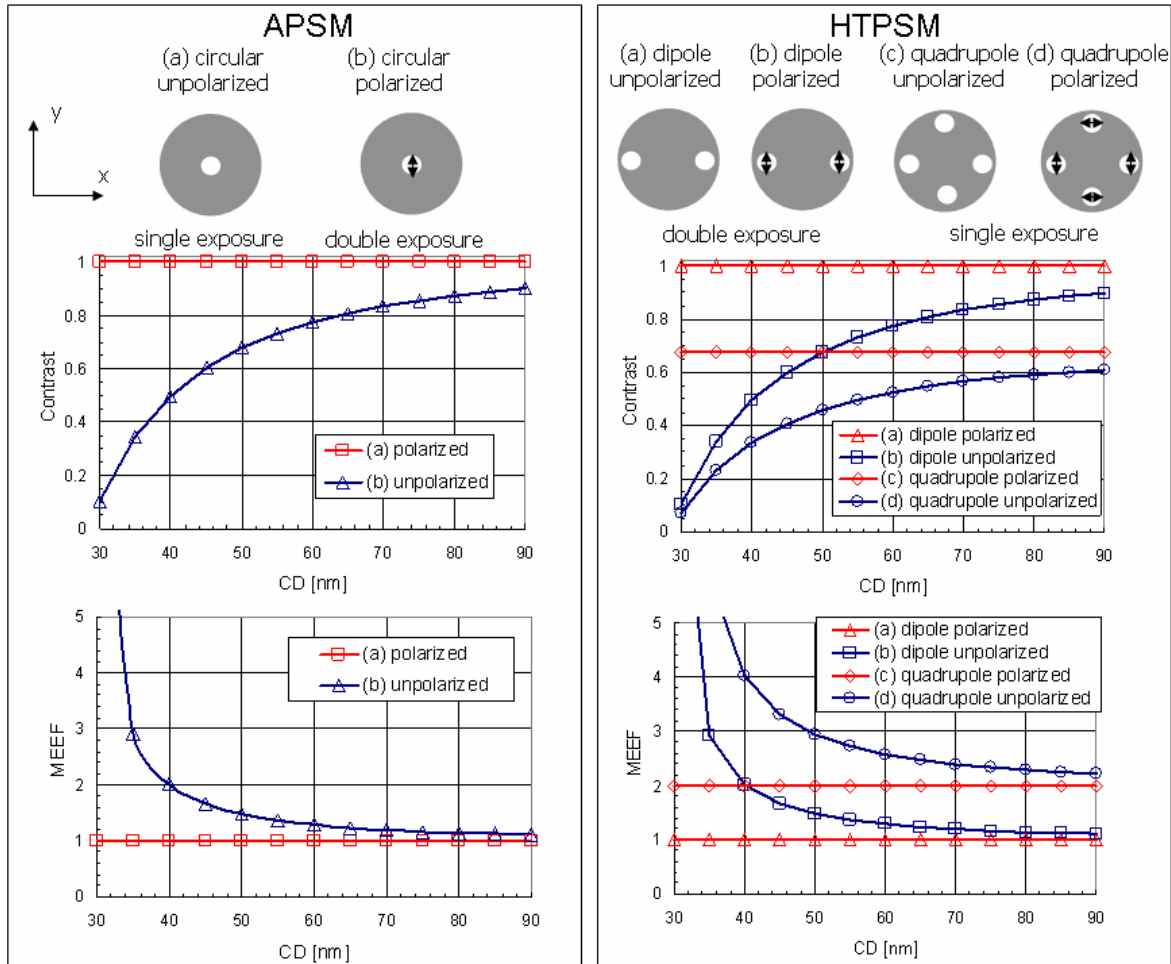


Figure 1: Comparison of printing of dense lines with APSM and HTPSM (6% transmission): MEEF and contrast for typical illumination conditions using polarized and un-polarized light; calculations are based on perfect two or three beam interference in resist  $n=1.7$ , infinitely thin masks with line/pitch=0.5 are assumed.

Printing of lines with APSM is conventionally performed with on axis illumination. Whereas for un-polarized light no special care needs to be taken for printing of structures in different directions, a linearly polarized circular illumination can be applied for structures in one direction only. In contrast to the off-axis illumination schemes using azimuthal or bipolar illumination, there is no obvious single exposure option using polarized light for APSM. This implies that, for gaining the benefit of polarized light, the design may need to be decomposed based on the orientation of the features or the orientation of the features may be restricted at the design phase by using for example restrictive design rules. In particular, for 2D features like contact holes, there is no apparent illumination scheme offering the benefits of polarized light.

It is useful to compare the printing options using unpolarized illumination first. Both contrast and MEEF for single exposure with unpolarized light (see Fig. 1) show a clear advantage for APSM. The application of an unpolarized dipole

illumination for HTPSM is, at least within the assumptions mentioned above, comparable to the performance of APSM but restricted to features in one direction.

This situation is somewhat different when polarized illumination is introduced. If the quadrupole illumination for HTPSM is combined with azimuthally polarized light, both contrast and MEEF become comparable to APSM unpolarized in the range 40-50nm half pitch and show better performance for smaller nodes. That means for 45nm applications the single exposure option using polarized light together with HTPSM may compete well with the unpolarized imaging of APSM. Comparing both double exposure options with polarized light, means dipole polarized and circular polarized, shows no obvious advantage for APSM in terms of both contrast and MEEF.

However, through pitch solutions show a different behavior. This is illustrated in Fig. 2, where the MEEF for APSM and HTPSM is compared for different pitches with polarized light. Here, the simulations were performed using SOLID E under the assumption of a perfectly thin mask. The influence of mask topography effects on MEEF are discussed in the next section. A 45nm line was analyzed for 3 different pitches using NA=1.35 with an immersion liquid n=1.44 and y (TE) polarized light. For the HTPSM mask, the dipole illumination was optimized at center partial coherence  $\sigma_{\text{center}}=0.8$  and a radius  $\sigma_{\text{radius}}=0.2$ . For the APSM mask we applied a circular illumination with a partial coherence of  $\sigma=0.2$ . To compare the inherent properties of both mask types the partial coherence values were chosen in such a way that for both mask types all diffraction orders are completely captured by the pupil. For all simulations the intensity inside the resist is considered. A resist model will certainly lead to an increase of the actual MEEF value. However, main focus here is the comparison between both mask types.

For a fixed pitch the intensity distribution is evaluated at different threshold levels resulting in different printed CD's. Plotted in Fig. 2 is the MEEF versus target CD for a fixed geometry. Whereas for dense lines the MEEF is comparable for polarized illumination, the advantage of APSM with respect to MEEF is clearly shown for larger pitches. At a target CD of 45nm the MEEF for APSM is less than half of the MEEF for HTPSM for both line to pitch ratios 1:3 and 1:4.

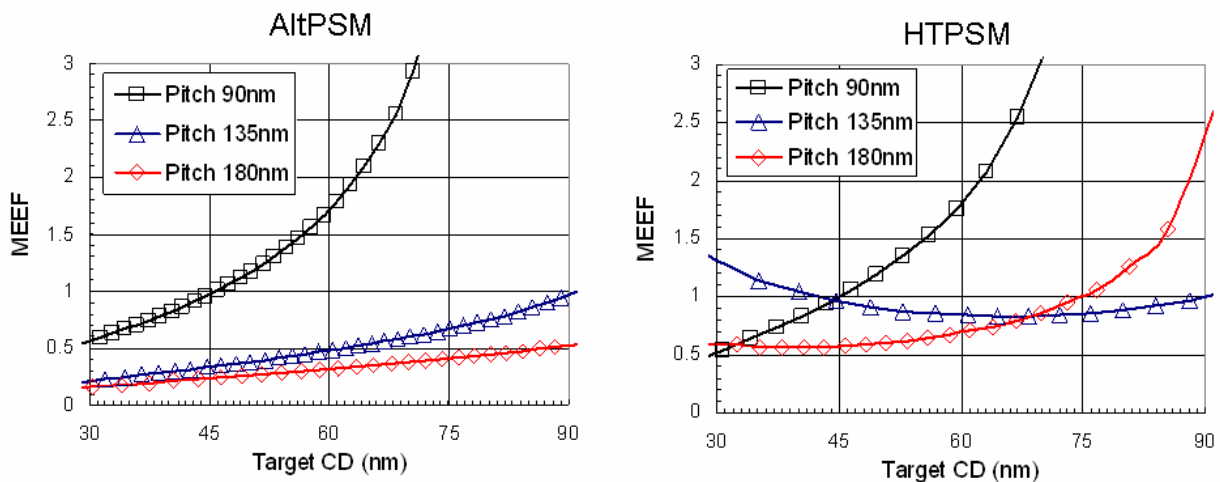


Figure 2: Comparison of MEEF for APSM and HTPSM for different pitches under y (TE) polarized illumination; depicted is MEEF versus Target CD corresponding to varying intensity thresholds; illumination settings are explained in text.

In particular the results obtained for dense lines imply that polarized illumination may be necessary for APSM to compete with HTPSM when printing sub 50nm half pitch patterns. The low sigma illumination conditions required for APSM constraints the choice of a possible polarized illuminator to the TE polarized option therefore limiting the patterns to be oriented in one direction.

Up to now perfectly thin masks were considered. However, it is important to investigate the influence of topography effects on APSM performance. In a recent study [11] it was shown that mask topography effects can significantly increase the MEEF for binary and APSM masks. Therefore, in the next subsection the influence of topography effects at small nodes is investigated. This study is quite relevant since the topography of the mask increase as the feature size is decreased while the quartz etch depth and the absorber thickness remain constant.

### 3. INFLUENCE OF MASK TOPOGRAPHY

#### Influence of Polarized Light on Balancing

It is well known that the application of APSM masks requires a balancing of neighboring features on mask, the reason being phase and transmission errors due to mask topography or non perfect mask fabrication. A number of correction schemes exist, among them pattern biasing or application of an undercut (see, for example [12]). It has been shown recently that the imbalance between neighboring features is also dependent on polarization [13]. It is therefore important to investigate balancing schemes with respect to their polarization properties.

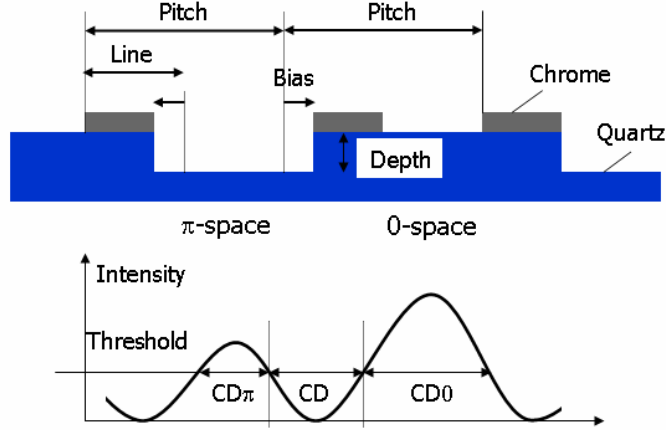


Figure 3: Alternating Phase Shifting Mask with line bias – definition of underlying geometry and relevant parameter.

Throughout the paper we will restrict ourselves to a simple balancing scheme based on a bias of the chrome line and an adjustment of the quartz etch depth. The underlying geometry is defined in Fig. 3. The offset is defined as the difference between the CDs of zero and pi shifted spaces in best focus, whereas the slope is the derivative of the CD difference with respect to defocus. The mask error enhancement factor is defined as the variation of the dark CD with respect to Chrome CD in best focus (both values given in wafer scale):

$$MEEF = \left. \frac{\partial CD}{\partial Line} \right|_{\text{BestFocus}}$$

For all rigorous simulations the optical lithography simulator SOLID E is used [14]. The mask is modeled using a full Maxwell equation solver based on the finite difference time domain (FDTD) method. As discussed in Section 2, to distinguish between mask topography and effects which may arise from resist processing we concentrate on the intensity in resist underneath the resist surface. Also, back reflections in the wafer stack are neglected by assuming an infinitely thick resist. As we are mainly interested in effects arising for half-pitches between 50nm and 40nm, an immersion fluid with refractive index of  $n=1.44$  is assumed. If not stated otherwise, all other settings are as in Section 2.

In a first step, the influence of polarized light on APSM balancing of dense lines is investigated. The balancing strategy is based on the mutual minimization of the offset and the slope by varying the line bias and the etch depth. Fig. 4 shows the optimum etch depth and line bias for dense lines and spaces with polarized and un-polarized illumination for varying half pitch on wafer.

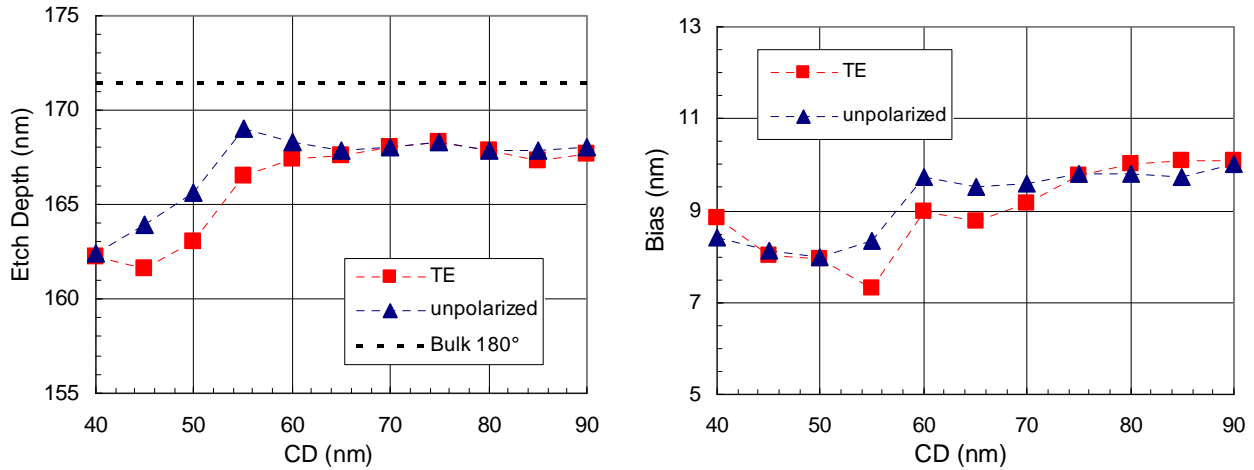


Figure 4: Optimum etch depth (mask scale) and bias (wafer scale) for dense lines and spaces versus wafer half pitch for polarized and un-polarized illumination.

It is found that for half pitches down to 60nm the lines can be balanced with a constant bias of around 10nm and an etch depth of 168nm. For smaller lines the structures show minimum offset and slope for a wider pi-space and shallower quartz etch. Whereas the line bias can easily be adapted by pattern dependent design rules, a pitch dependent etch depth is not trivial to compensate.

Comparing balancing between different polarization states shows significant deviations for structures smaller than 70nm half pitch. The difference in optimum bias can be as large as 4-5nm on the mask. More importantly, the effect of a required shallower etch depth is more pronounced for TE polarization. It is obvious from Fig. 4 that structures which are balanced for polarized light may show a significant imbalance for un-polarized light and vice versa. This is illustrated in Fig. 5, where the offset and slope are depicted for varying degree of polarization (DoP) for dense lines with 45nm and 65 nm half pitches. Whereas for 65nm half pitch the offset is largely affected by a variation of DoP, for 45nm half pitch the phase error is the main contributor to imbalance.

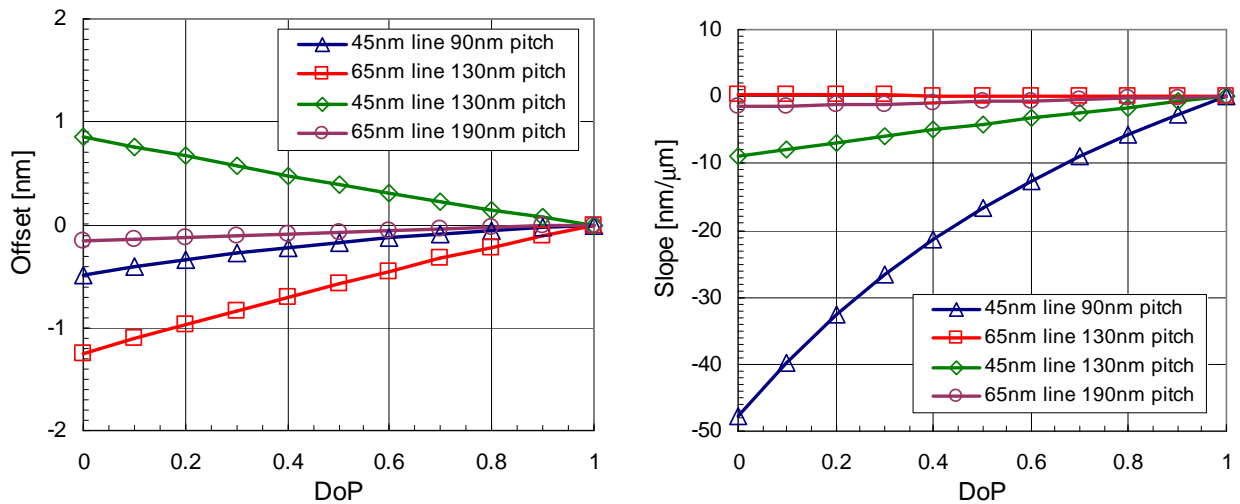


Figure 5: Slope and Offset versus Degree of Polarization for different line widths and pitches; lines are balanced for TE-polarized illumination (DoP=1); 45nm line NA=1.35, 65nm line NA=0.93,  $\sigma=0.2$ .

Another scenario particularly relevant for logic applications is the problem of balancing a fixed line through pitch. A corresponding simulation is shown in Fig. 6. Calculations were performed for 45 and 65nm wide lines, respectively. The differences in optimum etch bias for polarized and un-polarized light are rather small. For 45nm wide lines the line bias required is around 2-3nm smaller than for 65nm lines. The sharp decrease in optimum etch depth is observed for 45nm dense lines only. For larger pitches the required etch depth's are in the order of 168-171nm. The largest effects of polarization on optimum etch depth can also be seen for 45nm dense lines and spaces. For increasing pitch the polarization effects become smaller (see also Fig. 5). This implies that an increase of topography effects which manifest themselves in a variation of the required etch depth goes along with larger polarization effects.

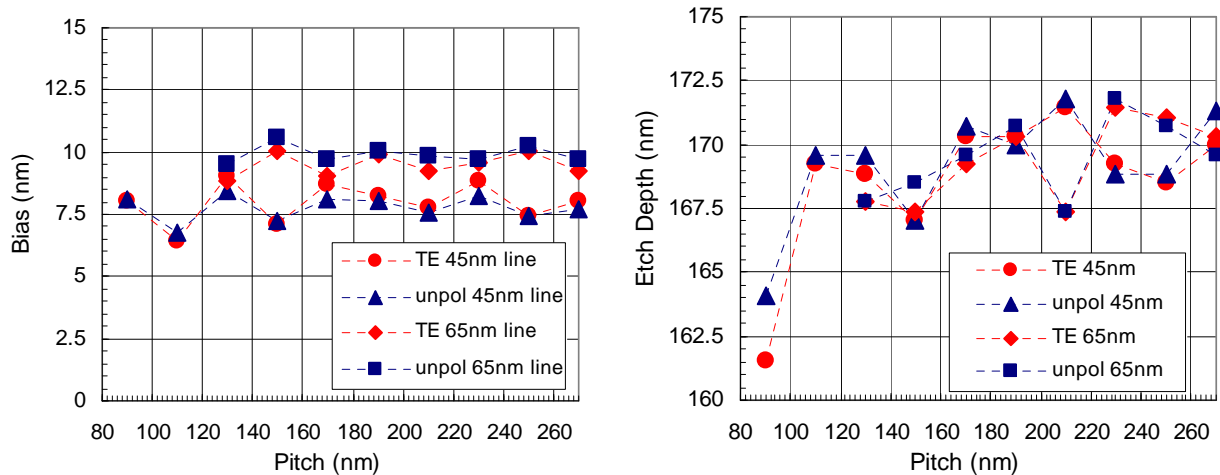


Figure 6: Optimum bias (wafer scale) and etch depth (mask scale) for fixed line (width 45nm and 65 nm) and varying pitch for polarized and un-polarized illumination.

From Fig. 4-6 it follows that the imbalance between neighboring features due to mask topography effects can depend on the polarization state of the exposing light. Main effects are observed for dense lines and spaces. This may have consequences on the mask making process. As an example, for verification of balancing in a mask shop an AIMS-tool is frequently used. The results obtained here entail that for an APSM mask which will be illuminated with polarized light also the AIMS-tool needs to be capable of handling polarized illumination.

### Influence of Topography on MEEF

In the preceding section it was shown that mask topography effects and, in particular, polarization effects increase for half pitches smaller than 60nm. As a small MEEF is considered to be one of the main advantages of APSM masks, it is interesting to investigate the influence of mask topography on MEEF. Fig. 7 shows the outcome of a corresponding simulation. Shown is the comparison between the Kirchhoff approximation and a rigorous simulation for varying pitches using polarized and un-polarized light. The width of the line of 45nm is fixed; all other settings and the evaluation procedure are as in Fig. 2 of Section 2.

For dense lines with a 90nm pitch and a target CD of 45nm, the MEEF simulated with mask topography is a factor of 1.2-1.3 larger than expected for a thin mask. For larger pitches, the effect becomes smaller and for a line to space ratio of around 1:3 the MEEF including topography is better than for a Kirchhoff mask. Interestingly, in this case the MEEF for polarized and un-polarized light is similar and there is no obvious benefit from using polarized light.

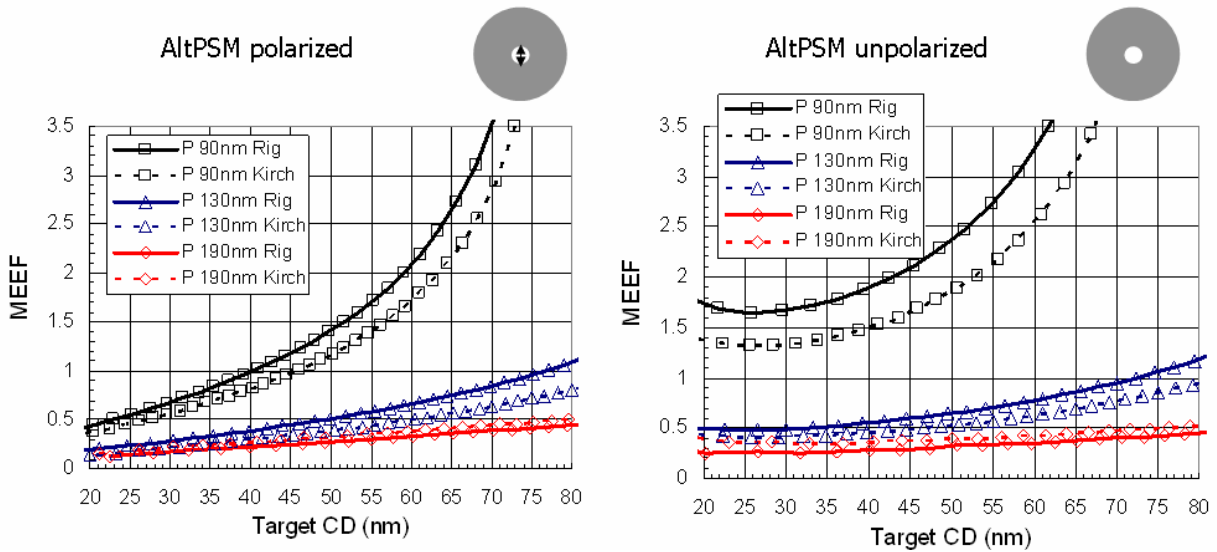


Figure 7: MEEF for APSM mask with fixed line width 45nm and different pitches 90/130/190nm: comparison between Kirchhoff approximation and rigorous simulation; NA=1.35,  $\sigma=0.2$ .

The topography effects shown here imply the use of polarization-dependant balancing of APSM. This should not be a show-stopper as long as it is properly handled at the time the mask is manufactured. Also, the MEEF is increased if compared to thin mask approximation but the relative numbers remain manageable. To further assess the usability of APSM in combination with polarized illumination, we need to consider the effect on the image quality of potential polarization errors in the illuminator.

#### 4. INFLUENCE OF POLARIZATION ERRORS

As was shown in the preceding sections, the topography effects of APSM masks show a certain degree of polarization dependence. This evokes the question how sensitive the printed CD is with respect to polarization errors of the source. It was shown in [4] that mask topography effects can enhance the sensitivity of CD variations to polarization errors, mainly because of polarization dependent transmission of the mask.

For an APSM mask, besides the actual CD the imbalancing and hence the displacement error is an important parameter which needs to be monitored. The displacement is given in terms of the CD's of the zero and pi-spaces as  $(CD_0 - CD_\pi)/4$ . It was shown in the preceding section that the balancing of an APSM mask varies with the polarization of the illumination. This could lead to a displacement error due to polarization errors of the source.

The analysis applied here follows the one in [4]. In Fig. 8 the CD over intensity threshold for dense lines is plotted for polarization rotation; shown is a comparison between APSM and HTPSM for both Kirchhoff approximation and a rigorous simulation. For the APSM rigorous simulation we have chosen a balanced structure with pattern bias as discussed in Section 3. The duty cycle for the HTPSM rigorous simulation is optimized to line/pitch=0.35. In both cases the half pitch is 45nm. All other parameters are as in Section 2 and 3.

For both APSM and HTPSM mask there exists a region of intersection, means an intensity threshold which shows no CD change with polarization. This so called iso-polarization point has been discussed in some detail in [4]. For both APSM and HTPSM mask the iso-polarization point is different for the rigorous simulation. Whereas for the Kirchhoff approximations the iso-polarization point nearly coincides with the iso-focal region, for the rigorous simulation the intersecting point moves away from the target resulting in larger CD errors. The transmission of the APSM mask decreases due to topography effects resulting in smaller thresholds for the target CD. The larger transmission and hence the higher intensity threshold for the HTPSM mask is due to the chosen bias of the line.

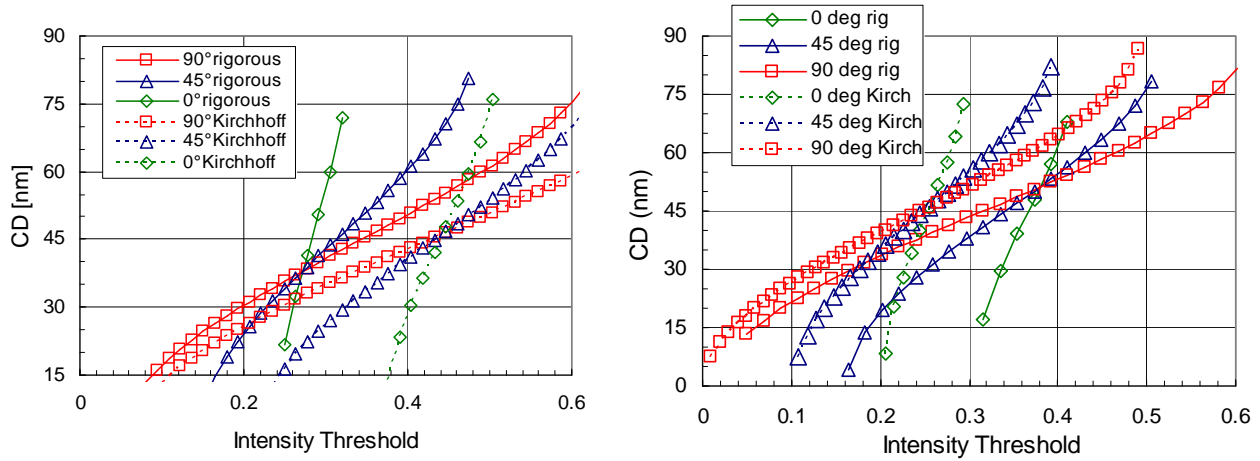


Figure 8: CD over intensity threshold for varying polarization rotation for APSM (on the left) and HTPSM (on the right) dense lines with half pitch 45nm; for both mask types a comparison between Kirchhoff approximation and rigorous simulation is shown. 90° and 0° correspond to TE and TM polarization, respectively.

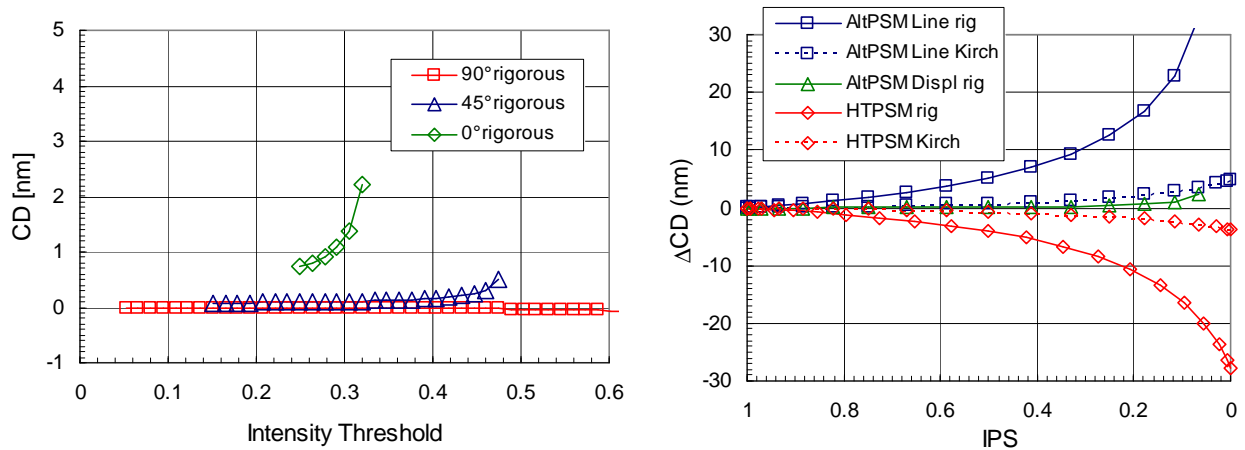


Figure 9: Left: Displacement over intensity threshold for varying polarization rotation – APSM mask; the mask is balanced for 90° (TE) polarization; Right: CD error and displacement versus intensity in the preferred state (IPS) for APSM and HTPSM mask – comparison between Kirchhoff approximation and rigorous simulation.

As discussed above, for an APSM mask the displacement is an additional parameter which needs to be monitored. In Fig. 9, the displacement versus intensity threshold for the same settings as in Fig. 8 is depicted. Note that the displacement for a Kirchhoff mask is always zero as the line is balanced for all polarization angles. The displacement for a topographical mask results from the polarization dependent balancing of the mask. The displacement error is small compared to the CD error of the dark line. This is shown in Fig. 9, where the CD and displacement errors are depicted versus the intensity in the preferred state (IPS). The IPS is defined as the percentage of light – polarized and unpolarized - in the targeted polarization state, here the TE or y-polarization. In [4] the IPS value was shown to be directly related to CD. However, the IPS in the simulations presented here was changed by a simple polarization rotation. The CD errors resulting from a topographical mask are much larger than for the Kirchhoff approximation, a fact that directly follows from Fig. 8. The displacement error is considerably smaller than the CD error of the dark line. A comparison between HTPSM and APSM shows similar CD errors but in opposite direction.



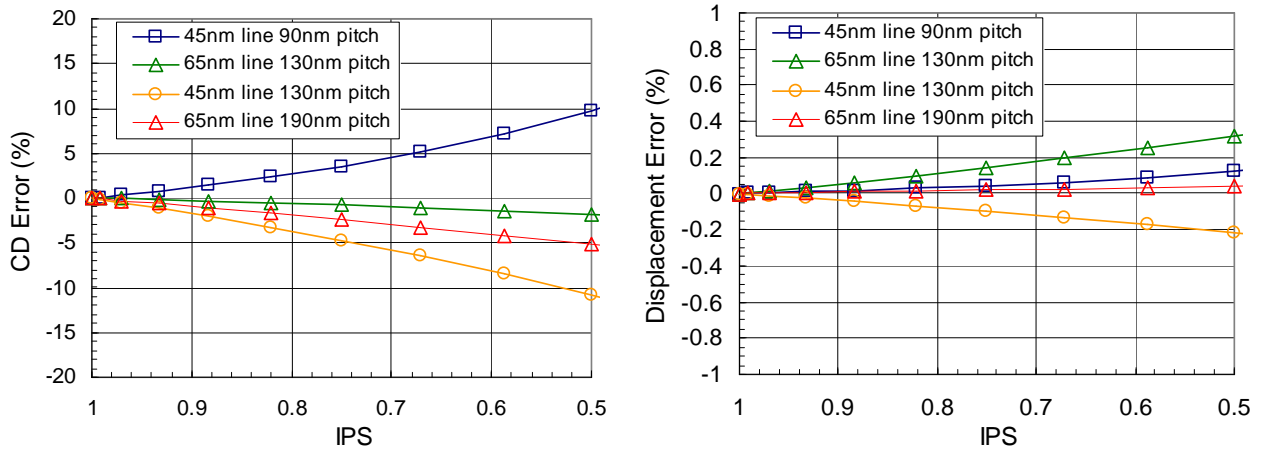


Figure 10: CD error and displacement over IPS for different line widths and pitches in best focus; the errors are relative to target CD's 45nm and 65nm, respectively; lines are balanced for TE-polarized illumination; 45nm lines NA=1.35, 65nm lines NA=0.93,  $\sigma=0.2$ .

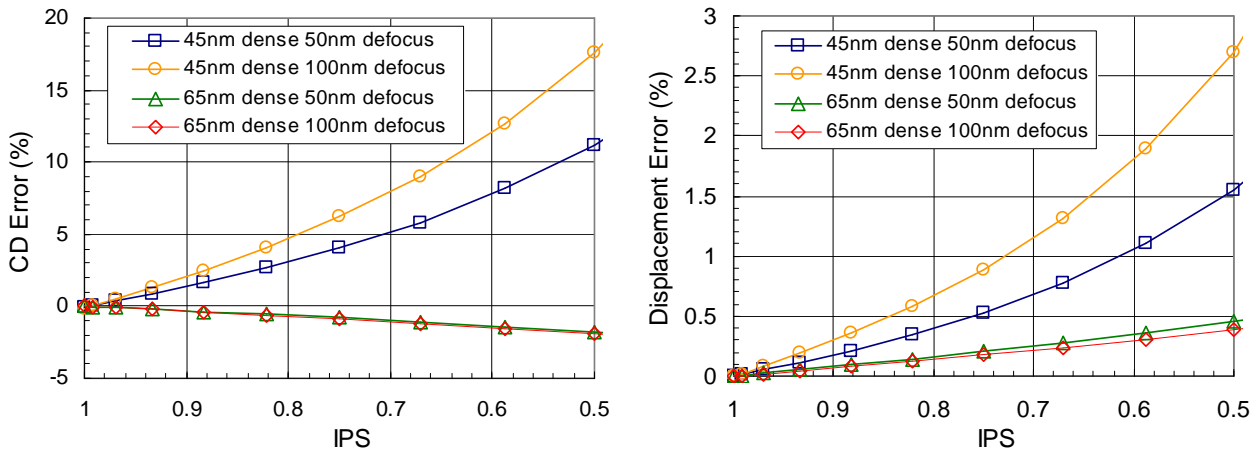


Figure 11: CD error (left) and displacement error (right) over IPS for 45nm and 65nm dense lines for 50nm and 100nm defocus, respectively; all other parameters as in Fig. 10.

Fig. 10 shows a comparison of CD error and displacement error versus IPS for different line widths and pitches. The 45nm lines show larger CD errors than 65nm lines. The displacement error in best focus is mainly driven by the polarization dependent bias of the structure. In Section 3 it was shown that 65nm dense lines show the largest sensitivity of optimum bias to polarization (see Fig. 4 and Fig. 6). This is in agreement with Fig. 10, where the largest displacement errors are found for 65nm dense lines. However, for all cases the displacement is much smaller than the CD variation of the dark line.

The large polarization effects on optimum etch depth observed for 45nm dense lines (see Fig. 4 and Fig. 5) should mainly result in a phase error and hence a displacement in defocus. Therefore the CD and displacement errors were calculated with 50nm and 100nm defocus, respectively. The results are shown in Fig. 11. Whereas the displacement error for 65nm dense lines is nearly unaffected, the polarization induced displacement for 45nm dense lines is much larger in defocus. Nevertheless, the CD variations are again more severe than displacement errors. This implies that polarization dependent transmission of the mask has more impact on the lithographic performance than polarization dependent balancing.

## 5. CONCLUSIONS

The use of Alternating Phase Shifting Masks with polarized light entails a number of problems. First of all, in contrast to off-axis illumination schemes there is no obvious solution for printing structures with different orientations in a single exposure. The same applies to the printing of real 2D structures like contact holes. The benefits of using APSM with un-polarized light compared to embedded phase shifting masks used with polarized light are small in the range of 40nm to 50nm half-pitch.

For typical double exposure options with polarized light, a comparison of HTPSM and APSM with respect to printing performance of dense lines and spaces shows similar MEEF and contrast. However, APSM shows advantages in terms of lower MEEF for through pitch imaging. Whereas for dense lines mask topography effects increase the MEEF, for large pitches the MEEF can actually be better than for a perfectly thin mask.

The optimum balancing of an APSM mask varies with polarization, which implies that balancing schemes need to be adjusted depending if polarized or un-polarized illuminations are used. Furthermore, metrology tools for balancing qualification like an AIMS tool need to be capable of handling polarized illumination.

The sensitivity of CD errors with respect to polarization errors of the source is comparable to HTPSM masks. The induced displacement error due to polarization errors is small compared to the CD variation of the dark line.

As the performance advantage of APSM is decreased compared to HTPSM and the manufacturing of APSM is complicated by polarization dependent light balancing, the option of using APSM becomes less attractive for sub 50nm half-pitch printing.

## ACKNOWLEDGEMENTS

This research was supported by the German Federal Ministry of Education and Research (BMBF) under contract No. 01M3154A (“Abbildungsmethodiken für nanoelektrische Bauelemente”).

## REFERENCES

1. B. W. Smith, J. Cashmore, “Challenges in high NA, polarization, and photoresists”, *Proceedings of the SPIE*, vol. 4691, pp. 11-24, 2002.
2. D. G. Flagello, et al., „Optical lithography in the sub-50nm regime“, *Proceedings of the SPIE*, vol. 5377, pp. 21-33, 2004.
3. B. W. Smith, L. Zavyalova, and A. Estroff, „Benefitting from polarization-effects on high-NA imaging“, *Proceedings of the SPIE*, vol. 5377, pp. 68-79, 2004.
4. D. G. Flagello, S. Hansen, B. Geh, and M. Totzeck, „Challenges with Hyper-NA (NA>1.0) Polarized Light Lithography for Sub  $\lambda/4$  resolution“, *Proceedings of the SPIE*, vol. 5754, pp. 21-33, 2005.
5. G. E. Bailey, Kostas Adam, „Polarization influences through the optical path“, *Proceedings of the SPIE*, vol. 5754, pp. 1102-1112, 2005.
6. R. Pforr, et al, „Polarized light for resolution enhancement at 70 nm and beyond“, *Proceedings of the SPIE*, vol. 5754, p. 92-106, 2005.
7. C. Kohler, et al, „Imaging enhancements by polarized illumination: theory and experimental verification“, *Proceedings of the SPIE*, vol. 5754, p. 734-750, 2005.
8. A. Estroff, Y. Fan, A. Bourov, B. W. Smith, „Mask-induced polarization effects at high numerical aperture“, *JM3 - Journal of Microlithography, Microfabrication, and Microsystems* 04 (03), 2005.
9. Bubke, et al, „ Investigation of polarization effects on new mask materials“, *Proceedings of the SPIE*, vol. 5754, p. 587-598, 2005.
10. Teuber, et al, „Determination of mask induced polarization effects occurring in hyper NA immersion lithography“, *Proceedings of the SPIE*, vol. 5754, p. 543-554, 2005.
11. Christophe Pierrat, Alfred K. Wong, „MEF revisited: low k1 effects versus mask topography effects“, *Proceedings of the SPIE*, vol. 5040, pp. 193-202, 2005.
12. D. J. Gerold, J. S. Peterson, and M. D. Levenson, „Multiple Pitch Transmission and Phase Analysis of Six Types of Strong Phase-Shifting Masks“, *Proceedings of the SPIE*, vol. 4346, pp. 729-743, 2001.
13. A. Erdmann, „Mask modeling in the low k1 and ultrahigh NA regime: phase and polarization effects“, *Proc. SPIE* Vol. 5835, p. 69-81, 21st European Mask and Lithography Conference, 2005.
14. SIGMA-C Product Site, <http://www.sigma-c.com>